A New Monofluorinated Phosphatidylcholine Forms Interdigitated Bilayers

Donald J. Hirsh,* Nancy Lazaro,# Lee R. Wright,# Joan M. Boggs,§ Thomas J. McIntosh,¶ Jacob Schaefer,* and Jack Blazyk#

*Department of Chemistry, Washington University, St. Louis, Missouri 63130 USA; #Department of Biomedical Sciences, College of Osteopathic Medicine, and Department of Chemistry and Biochemistry, College of Arts and Sciences, Ohio University, Athens, Ohio 45701 USA; §Department of Biochemistry, Research Institute, Hospital for Sick Children, and Department of Laboratory Medicine and Pathobiology, University of Toronto, Toronto, Ontario M5G 1X8, Canada; and ¶Department of Cell Biology, Duke University Medical Center, Durham, North Carolina 27710 USA

ABSTRACT 16-Fluoropalmitic acid was synthesized from 16-hydroxypalmitic acid using diethylaminosulfur trifluoride. This monofluorinated fatty acid then was used to make 1-palmitoyl-2-[16-fluoropalmitoyl]-phosphatidylcholine (F-DPPC) as a fluorinated analog of dipalmitoylphosphatidylcholine (DPPC). Surprisingly, we found that the phase transition temperature (T_m) of F-DPPC occurs near 50°C, ~10°C higher than its nonfluorinated counterpart, DPPC, as judged by both differential scanning calorimetry and infrared spectroscopy. The pretransition observed for DPPC is absent in F-DPPC. A combination of REDOR, rotational-echo double-resonance, and conventional solid-state NMR experiments demonstrates that F-DPPC forms a fully interdigitated bilayer in the gel phase. Electron paramagnetic resonance experiments show that below T_m, the hydrocarbon chains of F-DPPC are more motionally restricted than those of DPPC. X-ray scattering experiments confirm that the thickness and packing of gel phase F-DPPC is similar to that of heptanetriol-induced interdigitated DPPC. F-DPPC is the first phosphoglyceride containing sn-1 and sn-2 ester-linked fatty acyl chains of equal length that spontaneously forms interdigitated bilayers in the gel state in the absence of inducing agents such as alcohols.

INTRODUCTION

We have used rotational-echo double-resonance (REDOR) nuclear magnetic resonance (NMR) spectroscopy successfully to measure the proximity of a ^{13}C-labeled antimicrobial peptide to ^{31}P in the lipid polar headgroup, indicating the presence of significant surface interactions between the peptide and the lipid bilayer (Hirsh et al., 1996). This result, however, does not preclude the possibility that some fraction of the peptide may penetrate through the hydrophobic core of the membrane. To probe this region of the lipid bilayer, we first synthesized 16-fluoropalmitic acid, and then added the fluorinated fatty acid to the sn-2 position of 1-palmitoyl lysophosphatidylcholine to form 1-palmitoyl-2-[16-fluoropalmitoyl]-phosphatidylcholine (F-DPPC, see Fig. 1). By incorporating a single fluorine atom at the end of a fatty acyl chain in the lipids, our expectation was that these fluorines would reside near the center of the bilayer, thereby allowing the detection of dipolar couplings with ^{13}C-labeled peptides in their vicinity.

Fluorine-labeled fatty acids and phospholipids have served as useful NMR probes for studying biological membranes. Geminal difluoromethylene fatty acids can be incorporated into phospholipids biosynthetically (Pratt et al., 1983) or by chemical coupling at only the sn-2 (Dowd et al., 1984) or both the sn-1 and sn-2 (Post et al., 1984) positions. A serious drawback of lipids containing difluoromethylene groups is that bilayers containing these lipids often show evidence of phase separation (Dowd et al., 1993) or other perturbing effects (Oldfield et al., 1980).

Fatty acids containing only a single fluorine atom instead of two appear to be a preferable alternative. 16-Fluoropalmitic acid was incorporated biosynthetically into yeast plasma membranes (Esfahani et al., 1981) for ^{19}F-NMR experiments. Various monofluoropalmitic acids incorporated biosynthetically in *Acholeplasma laidlawii B* membranes were used to study the conformational state of membrane lipid acyl chains (Macdonald et al., 1985). The use of mono rather than difluorinated fatty acids causes less perturbation in lipid bilayers. McDonough et al. (1983) used monofluoropalmitic acids with a fluorine atom at position 5, 8, or 14 to synthesize bis-monofluoropalmitoyl-phosphatidylcholines. Aqueous multilamellar dispersions of these phospholipids showed that the fluorine substitutions have little effect on the thermotropic phase behavior of the lipid bilayers.

Thus, we expected that the single fluorine atom present in F-DPPC would not alter the physical properties of this lipid, in comparison with its parent compound, dipalmitoylphosphatidylcholine (DPPC). Using both differential scanning

Received for publication 12 November 1997 and in final form 24 June 1998.

Address reprint requests to Dr. Jack Blazyk, Department of Chemistry and Biochemistry, Ohio University, Athens, OH 45701. Tel.: 740-593-1742; Fax: 740-593-2320; E-mail: blazyk@ohiou.edu.

Nancy Lazaro's present address is Department of Chemistry, College of Science, De La Salle University, Manila, Philippines.

Lee R. Wright's present address is Department of Chemistry, Stanford University, Stanford, CA 94305.

Donald J. Hirsh's present address is The Liposome Company, Inc., One Research Way, Princeton, NJ 08540.

Part of this work was presented at the 41st Annual Meeting of the Biophysical Society and published in abstract form (Lazaro-Llanos et al., 1997).

0006-3495/98/10/1858/11 $2.00

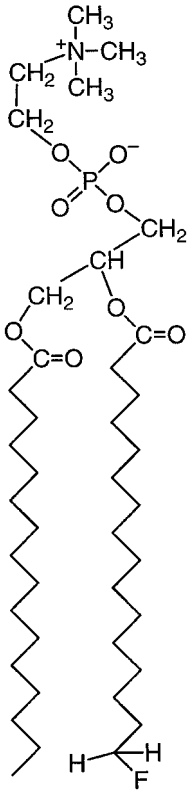

FIGURE 1 Structure of 1-palmitoyl-2-[16-fluoropalmitoyl]-phosphatidylcholine (F-DPPC).

calorimetry (DSC) and Fourier transform infrared (FTIR) spectroscopy, we found that the phase transition temperature (T_m) of F-DPPC is ~10°C higher than its nonfluorinated counterpart, and the pretransition characteristic of phosphatidylcholines is abolished. When REDOR NMR results for F-DPPC below T_m showed that the fluorine atoms at the end of the sn-2 chains are close to phosphorus and carbonyl and glycerol carbons, we concluded that F-DPPC must form interdigitated bilayers. Electron paramagnetic resonance (EPR) and x-ray diffraction studies support the conclusion that F-DPPC is interdigitated in the gel state. F-DPPC is the first phosphoglyceride with sn-1 and sn-2 ester-linked acyl chains of equal length that interdigitates spontaneously (i.e., without an inducing agent such as an alcohol).

MATERIALS AND METHODS

Synthesis of 16-fluoropalmitic acid and F-DPPC

16-Fluoropalmitic acid was synthesized from 16-hydroxypalmitic acid (Aldrich Chemical Co., Milwaukee, WI) using diethylaminosulfur trifluoride (Esfahani et al., 1981). The final product was purified by flash chromatography to give 90–95% of the acid as a white solid. ^{13}C-NMR δ 180.1214 (C-1), 34.0847 (C-2), 24.7651 (C-3), 29.5991 (C-14), 24.6457 (C-15), 85.1264 (C-16).

F-DPPC was synthesized from 16-fluoropalmitic acid by Avanti Polar Lipids, Inc. (Alabaster, AL). The fluorinated fatty acid was esterified to the sn-2 position of lysopalmitoylphosphatidylcholine to form F-DPPC. F-DPPC and DPPC were used as supplied from Avanti Polar Lipids, Inc. The purity of these compounds was confirmed by thin-layer chromatography.

FTIR spectroscopy

Lipid samples were hydrated with excess D_2O buffer (20 mM PIPES, 1 mM EGTA, pD 7.0) and incubated for at least 1 h at 60°C. Samples were applied to CaF_2 windows separated by a 25-μm Teflon spacer. Spectra were collected as a function of temperature using a Mattson Polaris FTIR spectrophotometer with a HgCdTe detector and a thermoelectrically controlled cell (Blazyk and Rana, 1987). A total of 250 interferograms were co-added and Fourier-transformed with triangular apodization to generate absorbance spectra with 2 cm^{-1} resolution and data points encoded every 1 cm^{-1}, with a signal-to-noise ratio of better than 500. Lipid phase changes were monitored by measuring the frequency of the symmetric methylene C–H stretching band as a function of temperature (Blazyk and Rana, 1987) using GRAMS/32 software (Galactic Industries, Inc., Salem, NH).

DSC

Sample cells containing 3–5 mg lipid and 50 μL buffer (20 mM PIPES, 1 mM EGTA, pH 7.0) in 100 μL stainless steel sample pans (Perkin-Elmer Corp., Norwalk, CT) were incubated at 60°C for at least 2 h before scanning. A reference cell contained 53 μL buffer in an identical sample pan. Thermograms were measured using a Perkin-Elmer Pyris 1 differential scanning calorimeter at a heating or cooling rate of 0.5°C/min. The amount of lipid present in the sample was determined by a phosphorus assay (Chen et al., 1956). The enthalpy of transition (ΔH_t) was determined using Pyris for Windows software (Perkin-Elmer Corp., Norwalk, CT). Curve fitting was performed using GRAMS/32 software (Galactic Industries, Inc.).

Solid-state NMR spectroscopy

Approximately 80 mg dry F-DPPC or DPPC was placed in a microcentrifuge tube. Buffer (20 mM HEPES, 1 mM EDTA, pH 7.0) was added at a 2:1 weight ratio, buffer to lipid, and the sample was heated at 60°C overnight with occasional vortex mixing. These liquid-crystalline lipid suspensions were allowed to cool to room temperature and the resulting gel phase suspension was packed into a 7-mm high-performance zirconia rotor with plastic (Kel-F) spacers and drive cap.

Experiments were run at 4.7 T using a wide-bore Oxford magnet (Oxford, UK). The pulse generator and acquisition system are from Tecmag (Houston, TX). Data acquisition was performed with a four-channel, transmission line probe, which permitted ^{19}F, ^{31}P, and ^{13}C detection or dephasing and ^{1}H and/or ^{19}F dipolar decoupling. The magic angle stators were from Chemagnetics (Fort Collins, CO). NMR spectra were acquired at a controlled magic-angle spinning (MAS) speed of 5000 Hz unless otherwise noted. Matched spin-locked cross-polarization (CP) was performed at 50 kHz for all ^{13}C and ^{19}F observe experiments. Typically, ^{13}C observe experiments used a 2-ms CP time and ^{1}H decoupling field strength of 94 kHz and a recycle delay of 2 s. ^{19}F observe experiments typically used a 4-ms CP time and ^{1}H decoupling field strength of 87 kHz. Unless otherwise noted, FID's were processed with 20 Hz line broadening before Fourier transformation. ^{13}C spectra were referenced to an external standard, the signal from the ^{13}C label of [4-^{13}C, 4-^{15}N]Asn set to 175.1 ppm. This external standard is in turn referenced to tetramethylsilane (TMS) at 0.0 ppm. ^{31}P spectra were also referenced to an external standard, the signal from phosphocreatine, set to 0.0 ppm. Unless otherwise noted, the temperature of F-DPPC was maintained at 30°C (gel phase) during data acquisition. For the spectrum of DPPC, the sample temperature was maintained at 13°C (gel phase) during data acquisition.

REDOR provides a direct measure of heteronuclear dipolar couplings, D_{IS}, between isolated pairs of labeled nuclei (Gullion and Schaefer, 1989b). In a solid with an I-S-labeled spin pair, for example, the S-spin rotational echoes that form each rotor period following a proton to S-spin

cross-polarization transfer can be prevented from reaching full intensity by insertion of one I-spin pi pulse and one S-spin pi pulse per rotor cycle. We use the convention here that S is the observed nucleus, ^{13}C, ^{19}F, or ^{31}P in these experiments. We refer to I as the dephasing nucleus since it is the I-spin's dipolar coupling with the S-spin that prevents the complete refocusing of the S-spin magnetization in the REDOR experiment. In these experiments the I spin is either ^{19}F or ^{31}P. The evolution period during which both I-spin and S-spin pi pulses are applied is referred to as the dephasing time.

In the REDOR experiment, one typically places the I-spin pi pulses in the middle of the rotor period and the S-spin pi pulses at the end of the rotor period to give the maximal attenuation of the S-spin magnetization for a given dephasing time. The dephasing time can then be lengthened or shortened to increase the difference between the intensity of the S-spin signal in the absence of I-spin pi pulses, the full echo spectrum (S_0), and the intensity of the S-spin signal in the presence of the I-spin pi pulses, the dephased spectrum (S). Because of the XY-8 phase-cycling scheme employed, the dephasing time is incremented in multiples of eight rotor cycles. The convention is to plot the difference spectrum, $\Delta S = S_0 - S$, above the full echo spectrum, S_0, and compare the ratio of the intensities in these two spectra, $\Delta S/S_0$, with the dephasing time to get the heteronuclear dipolar coupling, D_{IS} (Pan et al., 1990). Given D_{IS}, the internuclear distance, r_{IS}, can be easily calculated since D_{IS} is proportional to $(1/r_{IS})^3$.

In the two-dimensional version of REDOR that we call XDM, extended dipolar modulation, the dephasing time (i.e., the number of rotor cycles with both I-spin and S-spin pi pulses) is held fixed. Instead of changing the dephasing time, the placement of the I-spin pi pulse within the rotor period is incremented from near the beginning of the rotor period to near the end of the rotor period (Gullion and Schaefer, 1989a; Hing and Schaefer, 1993). The extent to which the I-S dipolar coupling interferes with refocusing of the S-spin magnetization is strongly dependent on the placement of the I-spin pi pulses. In this work, only the mirror-symmetric version of the XDM experiment was used, so that refocusing of S-spin magnetization would be unaffected by I-S scalar couplings (Gullion and Schaefer, 1989a; Hing and Schaefer, 1993).

In the XDM experiment one has finer control over the observed attenuation because the time increments can be made arbitrarily small. This makes it possible to measure accurately even relatively strong dipolar couplings, i.e., dipolar couplings in the kHz range (Hing and Schaefer, 1993). It also has the advantage, when comparing a series of measurements, that the dephasing time and the number of pi pulses on the I-spin and S-spin channels are held constant. The convention in the XDM experiment is to plot the ratio of the intensities of the signal obtained with and without I-spin pi pulses, S/S_0, versus the ratio t_1/T_r, where t_1 is the delay measured from the start of the rotor period at which the first I-spin pi pulse is applied and T_r is one rotor period.

EPR spectroscopy

The phosphatidylglycerol spin label, 1-palmitoyl-2-[16-doxylstearoyl]-phosphatidylglycerol (PG-SL), a kind gift from Dr. A. Watts, University of Oxford, was synthesized as described (Marsh and Watts, 1982). The fatty acid spin label, 5-doxyl-stearic acid (5-S-SL), was purchased from Syva (Palo Alto, CA).

Chloroform/methanol solutions of the lipids (0.5/sample) and spin label were combined at a molar ratio of 100:1 and the solvent was evaporated under a stream of nitrogen. After evacuation in a lyophilizer at ~0.1 torr for 2 h, 0.5 mL of 10 mM HEPES buffer containing 10 mM NaCl and 1 mM EDTA at pH 7.4 was added, and the sample was warmed to 65°C and dispersed by vigorous vortex mixing. Following centrifugation, all but ~50 μL of the supernatant was removed and the resuspended pellet was loaded into a 50-μL capillary tube. The capillary tube was sealed at one end with a torch and the tube was centrifuged at 2000 rpm.

EPR spectra were measured on a Varian E-104B spectrometer equipped with a Varian temperature controller and a DEC LSI-11 microcomputer system. All samples were heated to 57°C, a temperature above the phase transition temperature, just before measuring the sample in the gel phase at various temperatures. The maximum hyperfine splitting, $2T_{max}$, of the EPR spectra, calculated as shown in Boggs et al. (1989), was used as a measure of the degree of order and/or motional restriction of the probe in the lipids.

X-ray diffraction

For x-ray diffraction experiments, multilamellar vesicles of F-DPPC were prepared in excess buffer (10 0mM NaCl, 20 mM HEPES, pH 7.4) or the same buffer containing known concentrations of the neutral polymers, dextran (M_W = 500,000) or poly(vinylpyrrolidone) (PVP). The inclusion of these polymers in the buffer applies an "osmotic stress" to the lipid multilayers, thereby compressing the lamellar lattice and removing water from between apposing bilayers (Parsegian et al., 1979, 1986; McIntosh and Simon, 1986). The lipid suspensions were heated to 60°C three times for 30 min and extensively vortexed. The multilamellar lipid vesicles were concentrated by centrifugation with a bench centrifuge, sealed in thin-walled x-ray capillary tubes, and mounted in a point collimation x-ray camera as described previously (McIntosh and Simon, 1986). X-ray diffraction patterns were recorded on Kodak DEF x-ray film. X-ray films were processed by standard techniques and scanned with a Joyce-Loebl microdensitometer (McIntosh and Simon, 1986). After background subtraction, integrated intensities, $I(h)$, were obtained for each order h by measuring the area under each diffraction peak. For these unoriented patterns, the structure amplitude $F(h)$ was set equal to $\{h^2 I(h)\}^{1/2}$ (Blaurock and Worthington, 1966).

Electron density profiles, $\rho(x)$, on a relative electron density scale were calculated from

$$\rho(x) = (2/d)\sum \exp\{i\phi(h)\} \cdot F(h) \cdot \cos(2\pi xh/d)$$

where x is the distance from the center of the bilayer, d is the lamellar repeat period, $\phi(h)$ is the phase angle for order h, and the sum is over h. Phase angles were determined by comparing the observed structure amplitudes to those recorded previously for DPPC in both the normal lamellar ($L_{\beta'}$) and interdigitated lamellar ($L_{\beta I}$) phases (McIntosh et al., 1983; Simon and McIntosh, 1984; McIntosh and Simon, 1986). Electron density profiles described in this paper are at a resolution of $d/2h_{max} \approx 7$ Å.

RESULTS

DSC experiments

DSC heating and cooling curves comparing the phase behavior of DPPC and F-DPPC are shown in Fig. 2. The most striking difference between the two lipids is that the T_m of F-DPPC is ~10°C higher than that of DPPC. Phosphatidylcholines undergo a pretransition, in addition to the gel-to-liquid crystal phase change, which occurs near 35°C for DPPC (Mabrey and Sturtevant, 1976). This pretransition is associated with a change from the lamellar (gel) phase ($L_{\beta'}$), where the acyl chains undergo relatively slow rotational motion about their axis, to a hexagonal ripple phase ($P_{\beta'}$), with an accompanying increase in the area per chain that allows for faster rotation. The pretransition, which is evident in the heating curve for DPPC (Fig. 2 *A*), is absent for F-DPPC (Fig. 2 *C*).

In addition to the large difference in T_m, the width of the phase change is much greater for F-DPPC compared with DPPC. In Fig. 2 *C*, a shoulder is apparent on the endotherm in the heating curve for F-DPPC. The exotherm in the cooling curve for F-DPPC (Fig. 2 *D*) clearly contains at least two components. In Fig. 2 *C*, the endotherm in the heating curve for F-DPPC is resolved into two components

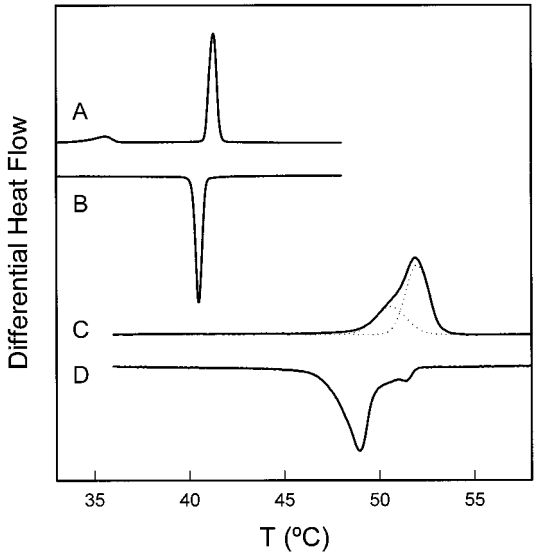

FIGURE 2 DSC thermograms for aqueous dispersions of DPPC and F-DPPC. (*A*) Heating curve for DPPC; (*B*) cooling curve for DPPC; (*C*) heating curve for F-DPPC; and (*D*) cooling curve for F-DPPC. The scan rate was 0.5°C/min in all cases. All thermograms were completely reversible. The endotherm in (*C*) was fitted with two Gaussian bands (*dotted curves*): one, centered at 50.6°C, accounts for 36% of the total area; the other, centered at 52.0°C, accounts for 64% of the total area.

by curve-fitting with Gaussian bands. The low-temperature component, centered at 50.6°C, and the high-temperature component, centered at 52.0°C, account for 36% and 64% of the total area, respectively. The significance and possible origin of the low-temperature component is discussed below.

The ΔH_t was calculated for the observed phase changes. For DPPC, the measured ΔH_t for the pretransition and main transition of 8.70 ± 0.05 kcal/mol agrees well with accepted literature values (Caffrey, 1993). For F-DPPC, the ΔH_t is substantially higher, with a value of 9.78 ± 0.06 kcal/mol. These values are essentially the same for both the heating endotherms and cooling exotherms.

FTIR experiments

Lipid phase changes were monitored by measuring changes in the frequency of the symmetric methylene C–H stretching band near 2850 cm^{-1} as a function of temperature. In the gel state, below T_m, the fatty acyl chains are extended and mostly in the *trans* conformation, and the lipid molecules are closely packed. Under these conditions, the C–H stretching band occurs at relatively low frequency (~2850 cm^{-1}). When the lipid bilayer undergoes the transition to the liquid-crystalline state, an increase in the proportion of *gauche* conformers in the acyl chain results in a less rigid structure, disruption of the tight packing of the chains, and greater intermolecular distance. The introduction of *gauche* conformers that gives rise to increased fluidity shifts the symmetric methylene C–H stretching band to a higher frequency (~2852–2853 cm^{-1}). Values of T_m can be estimated from the change in frequency of the C–H stretching band as a function of temperature (Blazyk and Rana, 1987).

Fig. 3 *A* shows the FTIR results overlaid with the calorimetric heating curve for DPPC. The frequency of the C–H stretching band is just above 2850 cm^{-1} near 33°C. A small increase in frequency accompanies the pretransition between 35 and 37°C, while a large increase in frequency coincides with the gel-to-liquid crystal endotherm between 40.5 and 42°C. In contrast, Fig. 3 *B* shows the same data for F-DPPC. The frequency of the C–H stretching band for F-DPPC is substantially lower than that of DPPC at all temperatures below the phase change. Moreover, the thermal event beginning below 50°C apparently is not the result of chain melting. The introduction of *gauche* conformers into the acyl chains does not begin until the temperature

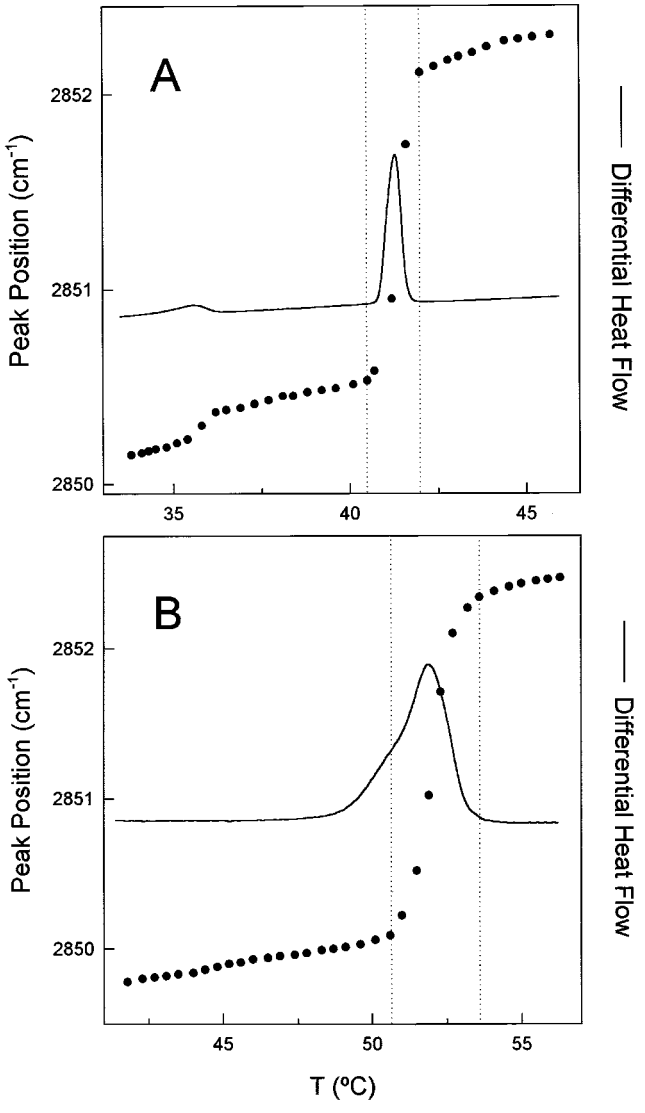

FIGURE 3 Phase changes monitored by the frequency of the symmetric methylene C–H stretching band as a function of temperature (●) for (*A*) DPPC and (*B*) F-DPPC. The solid lines are the DSC heating curves from Fig. 2. The vertical dotted lines represent the lower and upper limits of the transition from *trans* to *gauche* conformers in the hydrocarbon chains.

reaches nearly 51°C, as indicated by the vertical dotted lines showing the limits of the IR-detected phase change.

Solid-state NMR spectroscopy

The first indication that F-DPPC had an unusual morphology in the gel state came from ^{13}C observe, ^{19}F dephase REDOR experiments (Fig. 4). Significant dipolar couplings between fluorine and carbons in the acyl chain termini, carbons h–k, were expected for a normal bilayer phase and are observable as peaks in the difference spectrum, ΔS. However, peaks in the difference spectrum are also observed for carbons in or near the phospholipid headgroup, carbons c–g′, indicating that these carbons are also in proximity to fluorine. The assignment of resonances a–i in the full echo spectrum is based on the work of Lee and Griffin (1989). The assignment of resonances j and k is based our work (see Materials and Methods) and the relatively large peaks in the difference spectrum, ΔS, at the appropriate chemical shifts (Fig. 4).

If the fluorinated methyl terminus of the sn-2 fatty acyl chain of F-DPPC is in proximity to the carbons in the phospholipid headgroup, then it follows that it must also be near the phosphate group. There should then be an observable dipolar coupling between the phospholipid phosphorus (^{31}P) and the methyl terminus (^{13}C) of the fluorinated fatty acyl chain. To test this hypothesis, a ^{13}C observe, ^{31}P dephase REDOR experiment was performed on F-DPPC. The results are shown in Fig. 5. The difference spectrum, ΔS, shows peaks for the methyl carbons of both fatty acyl chains, fluorinated (j) and unfluorinated (i), indicating that these carbons are in proximity to the phosphorus in the phospholipid headgroup. Difference peaks are also observable from carbons in or near the phospholipid headgroup: a–g′. The same experiment was repeated with DPPC, which maintains a bilayer structure in the gel state (Fig. 5, *inset*). A peak in the difference spectrum at 14 ppm would indicate a significant dipolar coupling between the methyl carbons of the fatty acyl chains and the phospholipid phosphorus. None is observed.

It also follows that if the fluorinated methyl terminus of the sn-2 fatty acyl chain of F-DPPC is in proximity to the phospholipid headgroup, there should be observable ^{31}P–^{19}F dipolar couplings. This was confirmed by ^{19}F observe, ^{31}P dephase REDOR experiments (Fig. 6). The data points shown in the inset were obtained by varying the dephasing time in the REDOR experiment, i.e., the number of rotor cycles during which dephasing pulses were applied. The solid line shows the best fit to the data assuming a pairwise ^{19}F–^{31}P dipolar coupling. It is clear that the data deviate from this theoretical curve at long dephasing times (>10

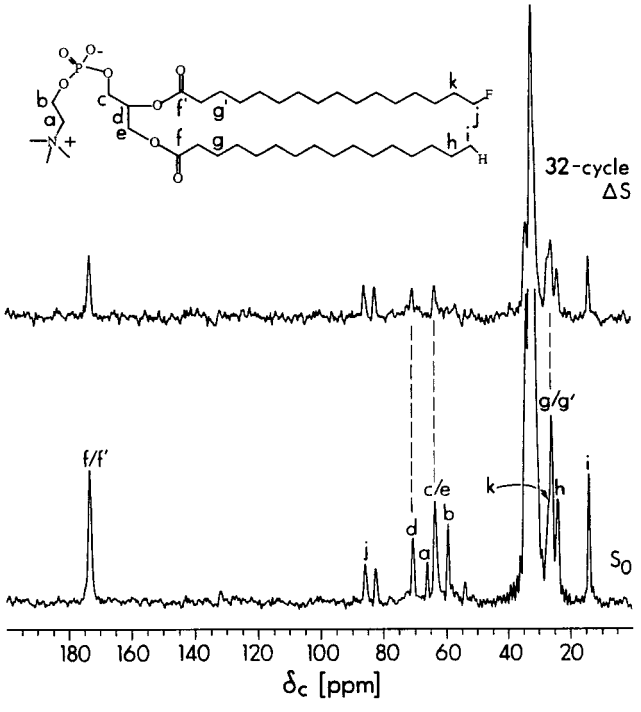

FIGURE 4 ^{13}C observe, ^{19}F dephase REDOR spectra of F-DPPC. Peaks in the difference spectrum, ΔS, arise from carbons which experience observable dipolar couplings with fluorine after 32 rotor cycles of ^{19}F dephasing. The resonance from the carbon directly bonded to fluorine, j, is split by its scalar coupling to fluorine. The number of scans accumulated for the full echo spectrum, S_0, was 9056.

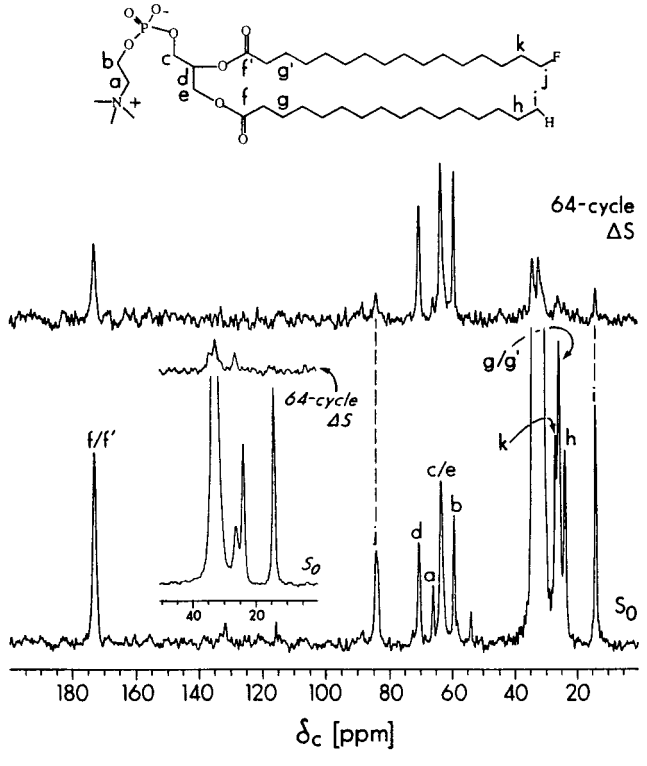

FIGURE 5 ^{13}C observe, ^{31}P dephase REDOR spectra of F-DPPC. The ^{13}C FID's were collected with both ^{1}H and ^{19}F decoupling so that the carbon directly bonded to fluorine gives a single resonance, j. *Inset:* ^{13}C observe, ^{31}P dephase REDOR spectra of DPPC in the gel state. Only the methyl and methylene resonances of the acyl chains of DPPC are shown. The numbers of scans accumulated for the full echo spectra were 16,000 (F-DPPC) and 40,832 (DPPC).

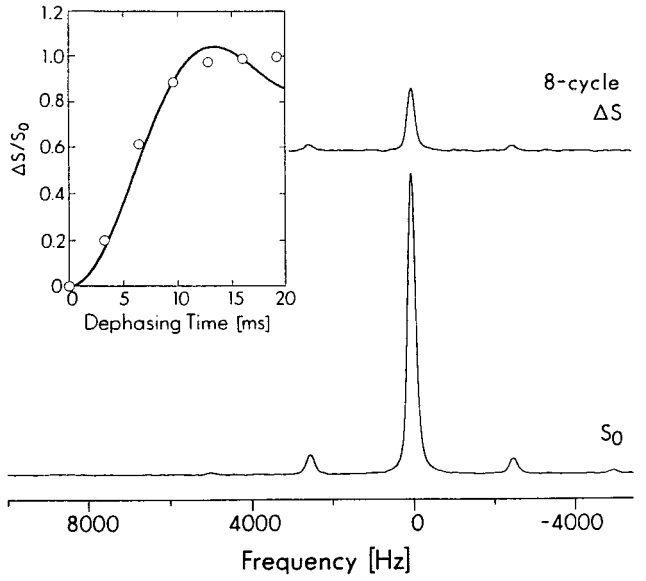

FIGURE 6 ^{19}F observe, ^{31}P dephase REDOR spectra of F-DPPC. *Inset:* Ratio of peak heights in the difference and full echo spectra, $\Delta S/S_0$, as a function of dephasing time. The point at $\Delta S/S_0 = 0.2$ corresponds to the spectrum at right. For a pairwise ^{19}F–^{31}P dipolar coupling, the best fit is shown by the solid curve. In these experiments a MAS speed of 2500 Hz was used. The number of scans collected for the full echo spectrum was 64. The FID's were processed with the equivalent of 80 Hz line broadening before Fourier transformation.

ms). A very similar curve was obtained when the REDOR experiment was reversed so that ^{31}P was the observe nucleus and ^{19}F was the dephase nucleus (data not shown).

One possible explanation for the difference between the ^{19}F observe, ^{31}P dephase REDOR data shown in Fig. 6 and that calculated for an isolated ^{19}F–^{31}P pair (*solid line*) is that each ^{19}F nucleus is coupled to more than one ^{31}P nucleus. To test this hypothesis and determine the minimum number of nuclei that would be required to model the ^{19}F dephasing behavior, the XDM experiment was used (Gullion and Schaefer, 1989a; Hing and Schaefer, 1993). The results of this experiment are shown by the black circles in Fig. 7. It is clear that a single pairwise ^{19}F–^{31}P dipolar coupling (*broken line*) does not adequately describe the data. Simulations for a fluorine atom dipolar coupled to two phosphorus atoms show that the dephasing behavior depends on the geometry. The simulation in which the three atoms, ^{31}P–^{19}F–^{31}P, form a right angle with fluorine at the vertex comes closest to fitting the data.

There are distinct ^{31}P lineshapes in nonspinning NMR spectra that are associated with the different phospholipid morphologies. The overall ^{31}P lineshape observed in the two spectra in Fig. 8 indicates that F-DPPC forms a lamellar phase at the temperatures investigated in this work. The top spectrum, taken at a temperature above the phase transition temperature, shows a small component with resonant frequencies near that of the isotropic chemical shift. This component disappears upon cooling to a temperature below the phase transition temperature and may arise from a subpopulation of small vesicles less than a micron in diameter.

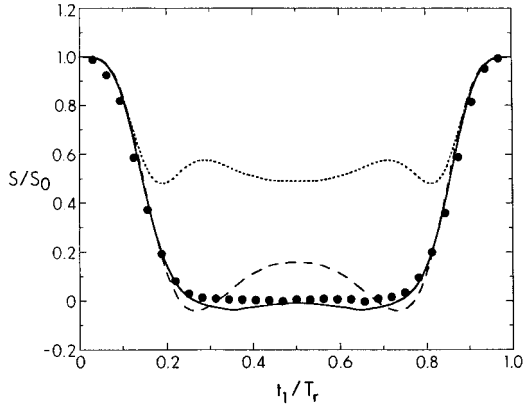

FIGURE 7 Results from a ^{19}F observe, ^{31}P dephase extended dipolar modulation (XDM) experiment on F-DPPC. The broken line represents the best fit assuming a pairwise ^{19}F–^{31}P dipolar coupling. The solid line and the dotted line represent simulations where each ^{19}F has dipolar couplings with two ^{31}P atoms, each 7.7 Å away. The simulation represented by the solid line assumes that the three atoms form a right angle with fluorine at the vertex, while the simulation represented by the dotted line assumes that the three atoms are co-linear with fluorine in the middle. Data acquisition and processing parameters were the same as that for Fig. 6 except that the number of rotor cycles of dephasing was fixed at 48 and the timing of the I-spin (^{31}P) pulses within the rotor period was varied.

The *trans/gauche* distribution of the fatty acyls chains can be estimated by examining the ^{13}C methylene resonances of the fatty acyl chains (Fig. 9). Methylene carbons in a *trans* configuration are expected to resonate at ~33 ppm while those in a *gauche* conformation are expected to resonate at ~30 ppm (Earl and Vander Hart, 1979). There is no distinct resonance at 30 ppm in this spectrum and very little intensity, indicating that both fatty acyl chains are in an

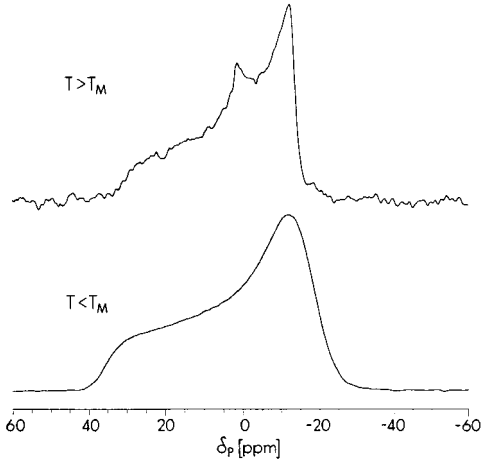

FIGURE 8 ^{31}P spectra of F-DPPC above the phase transition temperature, top spectrum, and below the phase transition temperature, bottom spectrum. The actual temperatures were 55°C and 30°C, respectively. The spectra were collected without MAS using a Hahn-echo sequence with an interpulse delay of 24 μs. The ^{31}P frequency field amplitude was 38 kHz and the data were collected with 50 kHz proton decoupling. The spectra resulted from the accumulation of 848 scans, top spectrum, and 24,048 scans, bottom spectrum. Before Fourier transformation, the FID's were processed with the equivalent of 80 Hz linebroadening.

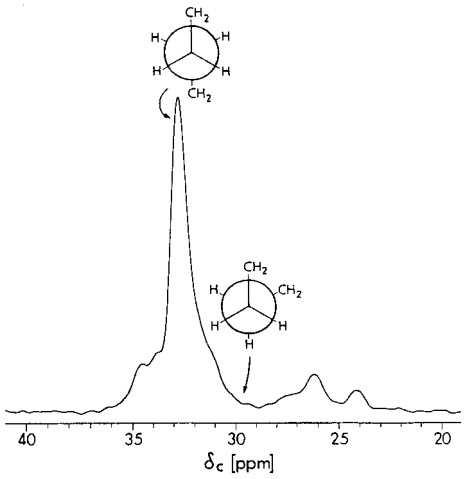

FIGURE 9 ^{13}C CP/MAS echo spectra of F-DPPC. For clarity, only that region of the spectrum where the methylene and methyl resonances of the fatty acyl chains appear is shown. The spectrum resulted from the accumulation of 1024 scans.

all-*trans* or nearly all-*trans* configuration. This conclusion also is supported by the low frequency of the C–H stretching vibrational band for F-DPPC (Fig. 3 *B*).

EPR experiments

The EPR spectra of PG-SL in DPPC and F-DPPC in the gel state (at 27.5°C) are shown in Fig. 10. The probe on carbon 16, near the end of the acyl chain, is clearly more motionally restricted in F-DPPC than in DPPC, with T_{max} values for F-DPPC and DPPC of 29.6 G and 22 G, respectively. In contrast, using 5-S-SL, where the probe is located much closer to the polar headgroup region, the T_{max} value at 27.5°C for F-DPPC (27.5 G) is much closer to that of DPPC (29.0 G). At 57°C, in the liquid crystalline phase, the T_{max} values of the fluorinated lipids were only slightly greater than those of the nonfluorinated lipids.

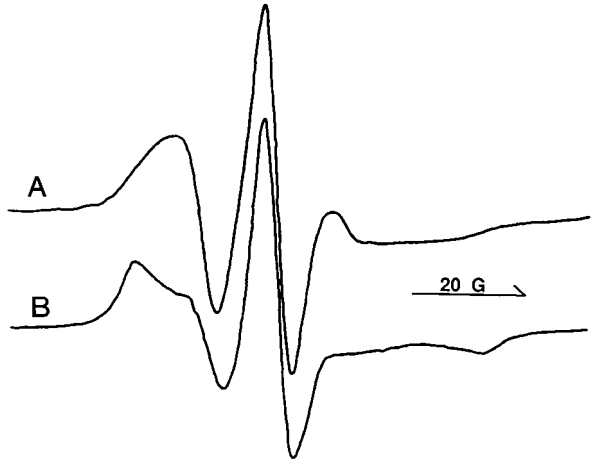

FIGURE 10 EPR spectra of 1-palmitoyl-2-[16-doxylstearoyl]-phosphatidylglycerol (PG-SL) at 27.5°C in aqueous dispersions of (*A*) DPPC and (*B*) F-DPPC.

X-ray diffraction

The diffraction patterns from all suspensions of F-DPPC consisted of a single sharp wide-angle reflection at 4.11 Å and three sharp low-angle reflections that indexed as the first three orders of a lamellar lattice. The observed low-angle repeat periods and structure factors are given in Table 1. The sharp wide-angle spacing, the low-angle repeat periods in buffer and polymer solutions, and the observed structure factors for the F-DPPC specimens were all very similar to those observed previously for multilayers of DPPC in the interdigitated ($L_{\beta I}$) phase (McIntosh et al., 1983; Simon and McIntosh, 1984; Simon et al., 1988).

The electron density profile of F-DPPC, shown in Fig. 11, was calculated assuming the same phase angles as previously determined for DPPC in the ($L_{\beta I}$) phase (McIntosh et al., 1983; Simon and McIntosh, 1984). For comparison, Fig. 11 also shows profiles of DPPC in buffer and a 3:1 mixture of DPPC and 1,2,3-heptanetriol (HTO). We have shown previously that DPPC in buffer is in the normal gel ($L_{\beta'}$) phase, whereas the addition of HTO (or other small amphipathic molecules such as ethanol or methanol) causes the hydrocarbon chains from apposing monolayers to fully interpenetrate or interdigitate, forming the ($L_{\beta I}$) phase (Simon and McIntosh, 1984; Simon et al., 1988). In each of the profiles in Fig. 11, the high density peaks (at ±15 Å for F-DPPC and 3:1 DPPC:HTO and at ±21 Å for DPPC) correspond to the lipid polar headgroups. The low density regions on the outer edges of each profile correspond to the fluid spaces between adjacent bilayers. For DPPC there is an electron density trough in the geometric center of the bilayer, indicating the localization of the low electron density terminal methyl groups in the bilayer center. In the DPPC profiles, between the headgroup peaks (at ±21 Å) and the terminal methyl trough in the center of the bilayer, are medium density regions that correspond to the methylene chains. For both F-DPPC and 3:1 DPPC:HTO there is no terminal methyl dip in the center of the bilayer and the hydrocarbon interior of the bilayer is considerably narrower than observed for DPPC. These structural features are characteristic of lipids in the interdigitated phase (Ranck et al., 1977; Ranck and Tocanne, 1982; McIntosh et al., 1983; Simon and McIntosh, 1984; Kim et al., 1987a, b).

TABLE 1 Repeat distances and structure factors for F-DPPC suspensions with increasing osmotic stress

Sample Preparation	Repeat Distance (Å)	F(1)	F(2)	F(3)
Excess Buffer*	50.2	—	—	—
5% Dextran	49.1	−2.01	−6.48	+1.72
15% PVP	47.1	−2.52	−5.40	+3.40
30% PVP*	46.7	—	—	—

*These two samples gave only two orders of diffraction.

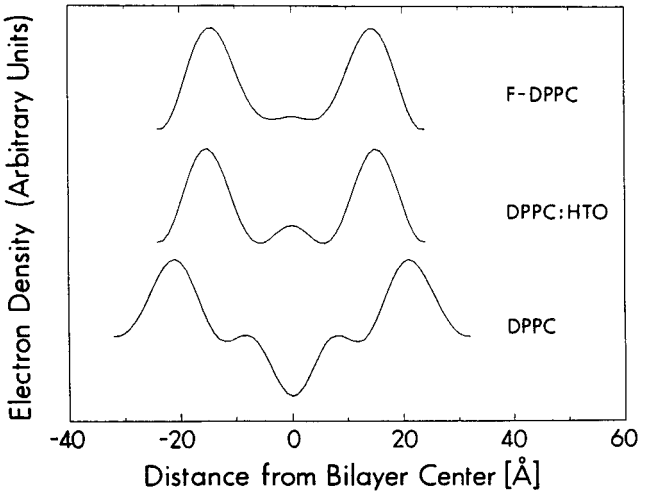

FIGURE 11 Electron density profiles of three gel-phase lipid systems: F-DPPC (*top*); 3:1 DPPC:1,2,3-heptanetriol (DPPC:HTO) (*middle*); and DPPC (*bottom*).

DISCUSSION

Sturtevant et al. (1979) incorporated geminal difluoromyristic acids substituted at positions 4, 8, or 12 at both the sn-1 and sn-2 positions to make tetrafluorinated phosphatidylcholines. Substitutions at positions 8 and 12 lowered T_m by 7°C and 4°C, respectively, while the geminal difluoro group at carbon 4 increased T_m by 5°C, as compared to dimyristoylphosphatidylcholine (DMPC). The ΔH_t values were all about twice that of DMPC. No pretransition was seen when the fluorine group was near the middle of the chain. Mixtures with DMPC all showed nonideal behavior. When these fluorinated fatty acids were incorporated only at the sn-2 position to make difluorinated lipids, substitutions at carbons 8 or 12 decreased T_m by ~10°C, while ΔH_t was unaffected; however, at carbon 4, there were two possible T_m and ΔH_t values (one higher and the other lower than those of DMPC), which depended on the thermal history of the sample (Dowd et al., 1993).

Monofluorinated fatty acids cause less perturbation to the lipid bilayer structure than geminal difluoromethylene-containing fatty acids. McDonough et al. (1983) studied the phase behavior of bis-monofluoropalmitoyl-phosphatidylcholines with fluorine at position 5, 8, or 14. All of these lipids showed decreases in T_m, ΔH_t, and pretransition temperature as compared to DPPC. The largest changes were observed for bis-[5-fluoropalmitoyl]-phosphatidylcholine, where T_m was lowered by 5°C and ΔH_t by 3.3 kcal/mol. The thermal properties of bis-[14-fluoropalmitoyl]-phosphatidylcholine were nearly identical to those of DPPC. These lipids exhibited ideal mixing with DPPC, where T_m and ΔH_t values were intermediate between the two pure components.

Because phosphatidylcholine with 14-fluoropalmitic acid substituted at both the sn-1 and sn-2 positions showed almost the same phase behavior as DPPC, we predicted that a single fluorine atom substitution on the terminal methyl carbon of palmitic acid at only the sn-2 position also would result in minimal perturbation. To our surprise, F-DPPC undergoes a gel-to-liquid crystal phase change which is more energetic and occurs at a much higher T_m than DPPC, and the pretransition is abolished. The observation that the frequency of the symmetric methylene C–H stretching band below T_m is consistently lower for F-DPPC as compared with DPPC suggests the possibility of more highly ordered acyl chains and enhanced stability of the gel state in the fluorinated lipid, although a direct effect by fluorine cannot be discounted.

The fact that F-DPPC does indeed adopt a bilayer structure was confirmed by ^{31}P-NMR (Fig. 8). The calorimetrically observed phase change for F-DPPC clearly contains at least two components (Fig. 2). Since the lower-temperature component does not correspond to the vibrationally detected change in conformation of the fatty acyl chains (Fig. 3 *B*), it must be the result of some other structural change in the lipid bilayer. Similar results were obtained in a dipalmitoylphosphatidylglycerol (DPPG)/polymyxin B mixture, where two endotherms comprised the calorimetric phase change (Kubesch et al., 1987) but only a single cooperative transition was detected by Raman and FTIR spectroscopy (Babin et al., 1987). In this case, polymyxin B induces interdigitation in DPPG in the gel state. The conversion of the interdigitated to noninterdigitated gel, which occurs at a lower temperature than the gel-to-liquid crystal transition, is accompanied by significant heat absorption but little change in acyl chain geometry.

A comparison of Figs. 2 *C* and 2 *D* reveals that the calorimetrically detected phase change in F-DPPC is not fully reversible. This observation, which is similar to the lack of reversibility associated with ethanol-induced interdigitation in saturated phosphatidylcholines (Rowe, 1985; Rowe and Cutrera, 1990), may result from differences in phase kinetics between heating and cooling. These data, however, are not sufficient to prove that F-DPPC forms interdigitated bilayers.

Our results from REDOR NMR experiments provided the first direct evidence that F-DPPC bilayers are interdigitated in the gel state. The proximity of fluorine to phosphorus and the glycerol carbons precluded the $L_{\beta'}$ or $P_{\beta'}$ structures typical of phosphatidylcholine below T_m (Fig. 12 *a*). The strong dipolar coupling between these nuclei is most easily explained by interdigitation (Fig. 12 *c*). The absence of *gauche* conformers in the fatty acyl chains, as judged by both FTIR and NMR, argues against intramolecular dipolar coupling that would arise from fluorine atoms approaching the polar headgroup in the same molecule. Such a sharp bend in the fatty acyl chain would require at least three methylene carbons to adopt a *gauche* conformation, as shown in Fig. 12 *b*.

The behavior of PG-SL in F-DPPC shown here is typical of its behavior in all interdigitated lipid bilayers we have studied and different from its behavior in noninterdigitated bilayers (Boggs et al., 1989). The similar or greater motional restriction of the probe at the 16th carbon of PG-SL,

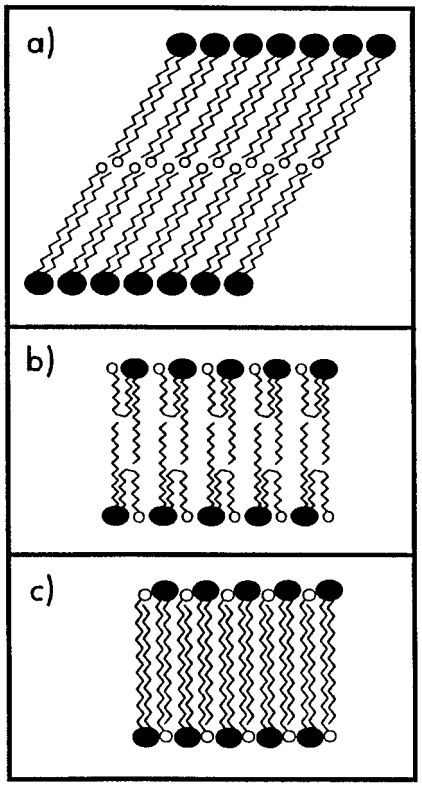

FIGURE 12 Diagram showing three possible molecular organizations of F-DPPC below T_m: (*a*) the $L_{\beta'}$ phase typical of nonfluorinated lipids such as DPPC; (*b*) a model in which the fluorinated fatty acyl chains are kinked so that the fluorine atoms are exposed at the surface of the bilayer; and (*c*) the $L_{\beta I}$ phase typical of interdigitated lipids.

compared with that of the probe located at the 5th carbon, in the fluorinated lipid indicates that the end of the fatty acyl chain is located near the interfacial region, suggesting the presence of an interdigitated bilayer (Boggs et al., 1981). A probe on the 16th carbon located in the center of a noninterdigitated bilayer normally has much greater motion than one on the 5th carbon, even in the gel phase, as observed for DPPC. Above T_m, the T_{max} values were typical of noninterdigitated liquid crystalline phase bilayers, suggesting that F-DPPC is not interdigitated in the liquid crystalline phase.

The x-ray diffraction data provide strong support that hydrated F-DPPC adopts an interdigitated ($L_{\beta I}$) phase below T_m. DPPC in the normal $L_{\beta'}$ gel phase has a repeat period of 63 Å and two wide-angle reflections, a sharp reflection at 4.2 Å and a broader band at ~4.1 Å (McIntosh, 1980). The sharp wide-angle reflection for F-DPPC is characteristic of bilayers with the hydrocarbon chains oriented perpendicular to the bilayer plane, as found in interdigitated bilayers (McIntosh et al., 1983; Simon and McIntosh, 1984; Kim et al., 1987a, 1987b). Fully hydrated suspensions of 3:1 DPPC:HTO in the interdigitated phase and F-DPPC have repeat periods near 50 Å and electron density profiles with the headgroup peaks at ±15 Å with no terminal methyl dip in the center of the profile (Fig. 11). Note that since DPPC:HTO and F-DPPC have essentially the same repeat periods and both of their electron density profiles show headgroup peaks at ±15 Å, it follows that adjacent bilayers are separated by ~20 Å in both DPPC:HTO and F-DPPC multilamellar vesicles. This distance corresponds to part of the headgroup from each apposing bilayer plus the fluid space between adjacent bilayers. So, the fluid spaces (and hydration levels) are approximately the same for DPPC:HTO and F-DPPC. Thus, the wide-angle reflections, the low-angle spacings, and the electron density profiles (Fig. 11) indicate that hydrated F-DPPC forms an interdigitated gel phase.

Interdigitation in phosphoglycerides with no chain length asymmetry can be induced by the addition of amphipathic molecules that accumulate at the interfacial region of the bilayer. These molecules can replace water and increase the surface area of the polar headgroups. Interdigitation in saturated phosphatidylcholines is precipitated by high concentrations of ethanol (Rowe, 1985; Nambi et al., 1988; Rowe and Cutrera, 1990). Glycerol induces interdigitation in DPPC, which results in an increase in T_m by 1°C and ΔH_t by 1.9 kcal/mol (Boggs and Rangaraj, 1985). Other larger alcohols such as HTO also induce interdigitation in DPPC (Simon and McIntosh, 1984). In addition to expanding the surface area of the bilayer, the alcohol molecules at the interface are probably protecting the ends of the fatty acyl chains from exposure to solvent and the polar environment of the surface.

Additionally, ions like thiocyanate cause DPPC to interdigitate, accompanied by a slight increase in T_m and the elimination of the pretransition (Cunningham et al., 1989). Dihexadecylphosphatidylcholine (DHPC) is an analog of DPPC in which the ester linkages between the hydrocarbon chains and the glycerol backbone are replaced by ether linkages. DHPC is known to form interdigitated bilayers in the gel phase, with a T_m ~2°C higher than that of DPPC, and a lower pretransition temperature (Ruocco et al., 1985).

Until now, all known interdigitation in symmetric phosphoglycerides has arisen from perturbations in the polar-nonpolar interface of the bilayer. How, then, does the presence of a single fluoride atom on the methyl group of the sn-2 acyl chain induce interdigitation? Other phosphatidylcholines containing fluorinated fatty acids do not appear to form interdigitated bilayers. For instance, the phase behavior of a DPPC analog containing 14-fluoropalmitic acid at both the sn-1 and sn-2 positions is nearly identical to that of DPPC (McDonough et al., 1983). Although 16-fluoropalmitic acid had been synthesized previously, it was not used to synthesize a DPPC analog; rather, it was biosynthetically incorporated into yeast plasma membranes (Esfahani et al., 1981). Perhaps the presence of fluorine at the end of the acyl chain is responsible for the unusual behavior of F-DPPC.

Several interesting fluorinated phosphatidylcholines, including a DPPC analog containing acyl chains in which carbons 13–16 are perfluorinated (F4C11PC), were synthesized for use as drug carriers (Santaella et al., 1991). These lipids form more stable liposomes for encapsulating doxorubicin (Frézard et al., 1994a) and carboxyfluorescein

(Frézard et al., 1994b) than their hydrogenated counterparts. Unlike F-DPPC, where T_m is increased and the pretransition is abolished, DSC results for these fluorinated lipids showed both pretransitions and main transitions at slightly lower temperatures and enthalpies than the corresponding hydrogenated phosphatidylcholines (Santaella et al., 1994). Furthermore, an electron density profile of gel phase F4C11PC clearly shows that the fluorine atoms are located at the center of the bilayer and that no interdigitation is observed (McIntosh et al., 1996). Thus, the presence of fluorine on the terminal carbon of the acyl chains is not sufficient to induce interdigitation in these bilayers.

The C–F bond in F-DPPC is strongly polarized due to the high electronegativity of the fluorine atom. The desire of this single strong dipole to be in contact with a polar environment may account for the energy to stabilize an interdigitated bilayer in the gel state. By exposing the dipole to water and other polar groups in the interfacial region, the free energy gain may be sufficiently large to drive the mutual insertion and stabilization of lipid molecules into the apposing monolayer. For F-DPPC, this can be achieved without any substantial change in acyl chain geometry. For other monofluorinated phosphatidylcholines where the fluorine atom is not at the end of the acyl chain, the facility of transferring the dipole to the surface of the bilayer might be hindered by the concomitant exposure of hydrocarbon to the polar region.

We have synthesized 1-palmitoyl-2-[16-fluoropalmitoyl]-phosphatidylglycerol, which also appears to be interdigitated in the gel state. Mixtures of F-DPPC and DPPC show phase behavior that is intermediate between the two pure lipids. Future experiments will explore the molecular organization of these lipids in greater detail. Finally, we plan to synthesize the 1,2-di-[16-fluoropalmitoyl]- and the 1-[16-fluoropalmitoyl]-2-oleoyl versions of phosphatidylcholine, phosphatidylglycerol, and phosphatidylethanolamine to determine the effects of fluorine in these lipids.

Simulations of the XDM data were performed using software developed by Christopher A. Klug, Ph.D.

This work was supported by grants from the Ohio University College of Osteopathic Medicine and Magainin Pharmaceuticals, Inc. (J.B.), and U.S. Public Health Service Grants GM-51554 (to J.S.) and GM-27278 (to T.J.M.). D.J.H. was supported by a National Research Service Award (#5F32AI09135) from the National Institute of Allergy and Infectious Disease.

REFERENCES

Babin, Y., J. D'Amour, M. Pigeon, and M. Pézolet. 1987. A study of the structure of polymyxin B-dipalmitoylphosphatidylglycerol complexes by vibrational spectroscopy. *Biochim. Biophys. Acta*. 903:78–88.

Blaurock, A. E., and C. R. Worthington. 1966. Treatment of low angle x-ray data from planar and concentric multilayered structures. *Biophys. J.* 6:305–312.

Blazyk, J., and F. R. Rana. 1987. An automated temperature control and data acquisition system for Fourier transform infrared studies: application to phase changes in hydrocarbons and lipid bilayers. *Appl. Spectrosc.* 41:40–44.

Boggs, J. M., and G. Rangaraj. 1985. Phase transitions and fatty acid spin label behavior in interdigitated lipid phases induced by glycerol and polymyxin. *Biochim. Biophys. Acta*. 816:221–233.

Boggs, J. M., G. Rangaraj, and A. Watts. 1989. Behavior of spin labels in a variety of interdigitated lipid bilayers. *Biochim. Biophys. Acta*. 981: 243–253.

Boggs, J. M., D. Stamp, and M. A. Moscarello. 1981. Interaction of myelin basic protein with dipalmitoylphosphatidylglycerol: dependence on the lipid phase and investigation of a metastable state. *Biochemistry*. 20: 6066–6072.

Caffrey, M. 1993. LIPIDAT: A Database of Thermodynamic Data and Associated Information on Lipid Mesomorphic and Polymorphic Transitions. CRC Press, Boca Raton, FL. 71–102.

Chen, P. S., T. Y. Toribara, and H. Warner. 1956. Microdetermination of phosphorus. *Anal. Chem.* 28:1756–1758.

Cunningham, B. A., W. Tamura-Lis, L. J. Lis, and J. M. Collins. 1989. Thermodynamic properties of acyl chain and mesophase transitions for phospholipids in KSCN. *Biochim. Biophys. Acta*. 984:109–112.

Dowd, S. R., V. Simplaceanu, and C. Ho. 1984. Fluorine-19 nuclear magnetic resonance investigation of fluorine-19-labeled phospholipids. 2. A line-shape analysis. *Biochemistry*. 23:6142–6146.

Dowd, S. R., J. M. Sturtevant, V. Simplaceanu, and C. Ho. 1993. ^{31}P-NMR and calorimetric studies of the low-temperature behavior of three ^{19}F-labeled dimyristoylphosphatidylcholines. *J. Phys. Chem.* 97:2946–2951.

Earl, W. L., and D. L. Vander Hart. 1979. Observations in solid polyethylene by carbon-13 NMR with MAS. *Macromolecules*. 12:762–767.

Esfahani, M., J. R. Cavanaugh, P. E. Pfeffer, D. W. Luken, and T. M. Devlin. 1981. ^{19}F-NMR and fluorescence polarization of yeast plasma membrane and isolated lipids. *Biochem. Biophys. Res. Commun.* 101: 306–311.

Frézard, F., C. Santaella, M.-J. Montisci, P. Vierling, and J. G. Riess. 1994a. Fluorinated phosphatidylcholine-based liposomes: H^+/Na^+ permeability, active doxorubicin encapsulation and stability in human serum. *Biochim. Biophys. Acta*. 1194:61–68.

Frézard, F., C. Santaella, P. Vierling, and J. G. Riess. 1994b. Permeability and stability in buffer of fluorinated phospholipid-based liposomes. *Biochim. Biophys. Acta*. 1192:61–70.

Gullion, T., and J. Schaefer. 1989a. Detection of weak heteronuclear dipolar coupling by rotational-echo double resonance. *Adv. Magn. Reson.* 13:57–83.

Gullion, T., and J. Schaefer. 1989b. Rotational echo double-resonance NMR. *J. Magn. Reson.* 81:196–200.

Hing, A. W., and J. Schaefer. 1993. Two-dimensional rotational-echo double resonance of Val_1-[1-^{13}C]Gly_2-[^{15}N]Ala_3-gramicidin A in multilamellar dimyristoylphosphatidylcholine dispersions. *Biochemistry*. 32: 7593–7604.

Hirsh, D. J., J. Hammer, W. L. Maloy, J. Blazyk, and J. Schaefer. 1996. Secondary structure and location of a magainin analog in synthetic phospholipid bilayers. *Biochemistry*. 35:12733–12741.

Kim, J. T., J. Mattai, and G. G. Shipley. 1987a. Bilayer interactions of ether- and ester-linked phospholipids: dihexadecyl- and dipalmitoylphosphatidylcholines. *Biochemistry*. 26:6599–6603.

Kim, J. T., J. Mattai, and G. G. Shipley. 1987b. Gel phase polymorphism in ether-linked DHPC bilayers. *Biochemistry*. 26:6592–6598.

Kubesch, P., J. Boggs, L. Luciano, G. Maass, and B. Tümmler. 1987. Interaction of polymyxin B nonapeptide with anionic phospholipids. *Biochemistry*. 26:2139–2149.

Lazaro-Llanos, N., D. J. Hirsh, J. Schaefer, and J. Blazyk. 1997. Phase behavior of fluorinated phosphoglycerides: can a single fluorine atom induce interdigitation? *Biophys. J.* 72:69*a*. (Abstr.).

Lee, C. W. B., and R. G. Griffin. 1989. Two-dimensional ^{1}H/^{13}C heteronuclear chemical shift correlation spectroscopy of lipid bilayers. *Biophys. J.* 55:355–358.

Mabrey, S., and J. M. Sturtevant. 1976. Investigation of phase transitions of lipids and lipid mixtures by high sensitivity differential scanning calorimetry. *Proc. Natl. Acad. Sci. USA*. 73:3862–3866.

Macdonald, P. M., B. D. Sykes, R. N. McElhaney, and F. D. Gunstone. 1985. ^{19}F NMR studies of lipid fatty acyl chain order and dynamics in *Acholeplasma laidlawii B* membranes. Orientational order in the pres-

ence of a series of positional isomers of cis-octadecenoic acid. *Biochemistry*. 24:177–184.

Marsh, D., and A. Watts. 1982. Spin labeling and lipid-protein interactions in membranes. *In* Lipid-Protein Interactions, Vol. 2. P. C. Jost and O. H. Griffith, editors. Wiley-Interscience, New York. 53–126.

McDonough, B., P. M. Macdonald, B. D. Sykes, and R. N. McElhaney. 1983. Fluorine-19 nuclear magnetic resonance studies of lipid fatty acyl chain order and dynamics in *Acholeplasma laidlawii B* membranes. A physical, biochemical, and biological evaluation of monofluoropalmitic acids as membrane probes. *Biochemistry*. 22:5097–5103.

McIntosh, T. J. 1980. Differences in hydrocarbon chain tilt between hydrated phosphatidylethanolamine and phosphatidylcholine bilayers: a molecular packing model. *Biophys. J.* 29:237–246.

McIntosh, T. J., R. V. McDaniel, and S. A. Simon. 1983. Induction of an interdigitated gel phase in fully hydrated lecithin bilayers. *Biochim. Biophys. Acta*. 731:109–114.

McIntosh, T. J., and S. A. Simon. 1986. The hydration force and bilayer deformation: a reevaluation. *Biochemistry*. 25:4058–4066.

McIntosh, T. J., S. A. Simon, P. Vierling, C. Santaella, and V. Ravily. 1996. Structure and interactive properties of highly fluorinated phospholipid bilayers. *Biophys. J.* 71:1853–1868.

Nambi, P., E. S. Rowe, and T. J. McIntosh. 1988. Studies of the ethanol-induced interdigitated gel phase in phosphatidylcholines using the fluorophore 1,6-diphenyl-1,3,5-hexatriene. *Biochemistry*. 27:9175–9182.

Oldfield, E., R. W. K. Lee, M. Meadows, S. R. Dowd, and C. Ho. 1980. Deuterium NMR of specifically deuterated fluorine spin probes. *J. Biol. Chem.* 255:11652–11655.

Pan, Y., T. Gullion, and J. Schaefer. 1990. Determination of C-N internuclear distances by rotational-echo double-resonance NMR of solids. *J. Magn. Reson.* 90:330–340.

Parsegian, V. A., N. Fuller, and R. P. Rand. 1979. Measured work of deformation and repulsion of lecithin bilayers. *Proc. Natl. Acad. Sci. USA*. 76:2750–2754.

Parsegian, V. A., R. P. Rand, N. L. Fuller, and R. C. Rau. 1986. Osmotic stress for the direct measurement of intermolecular forces. *Methods Enzymol.* 127:400–416.

Post, J. F. M., B. W. Cook, S. R. Dowd, I. J. Lowe, and C. Ho. 1984. Fluorine-19 nuclear magnetic resonance investigation of fluorine-19-labeled phospholipids. 1. A multiple-pulse study. *Biochemistry*. 23: 6138–6141.

Pratt, E. A., J. A. Jones, P. F. Cottam, S. R. Dowd, and C. Ho. 1983. A biochemical study of the reconstitution of D-lactate dehydrogenase-deficient membrane vesicles using fluorine-labeled components. *Biochim. Biophys. Acta*. 729:167–175.

Ranck, J. L., T. Keira, and V. Luzzati. 1977. A novel packing of the hydrocarbon chains in lipids. The low temperature phase of DPPG. *Biochim. Biophys. Acta*. 488:432–441.

Ranck, J. L., and J. F. Tocanne. 1982. Choline and acetylcholine induce interdigitation of hydrocarbon chains in DPPG lamellar phase with stiff chains. *FEBS Lett.* 143:171–174.

Rowe, E. S. 1985. Thermodynamic reversibility of phase transitions. Specific effects of alcohols on phosphatidylcholines. *Biochim. Biophys. Acta.* 813:321–330.

Rowe, E. S., and T. A. Cutrera. 1990. Differential scanning calorimetric studies of ethanol interactions with distearoylphosphatidycholine: transition to the interdigitated phase. *Biochemistry*. 29:10398–10404.

Ruocco, M. J., D. J. Siminovitch, and R. G. Griffin. 1985. Deuterium NMR investigation of ether- and ester-linked phosphatidylcholine bilayers. *Biochemistry*. 24:2406–2411.

Santaella, C., P. Vierling, and J. G. Riess. 1991. New perfluoroalkylated phospholipids as injectible amphiphiles. Synthesis, preliminary physicochemical and biocompatibility data. *New J. Chem.* 15:685–692.

Santaella, C., P. Vierling, J. G. Riess, T. Gulik-Krzywicki, A. Gulik, and B. Monasse. 1994. Polymorphic phase behavior of perfluoroalkylated phosphatidylcholines. *Biochim. Biophys. Acta*. 1190:25–39.

Simon, S. A., and T. J. McIntosh. 1984. Interdigitated hydrocarbon chain packing causes the biphasic transition behavior in lipid/alcohol suspensions. *Biochim. Biophys. Acta*. 773:169–172.

Simon, S. A., T. J. McIntosh, and A. D. Magid. 1988. Magnitude and range of the hydration pressure between lecithin bilayers as a function of head group density. *J. Colloid Interface Sci.* 126:74–83.

Sturtevant, J. M., C, Ho, and A. Reimann. 1979. Thermotropic behavior of some fluorodimyristoylphosphatidylcholines. *Proc. Natl. Acad. Sci. USA*. 76:2239–2243.